ISSN 0016-7029, Geochemistry International, 2006, Vol. 44, No. 2, pp. 137–142. © Pleiades Publishing, Inc., 2006.
Original Russian Text © L.V. Sazonova, V.I. Fel'dman, E.A. Kozlov, N.A. Dubrovinskaya, L.S. Dubrovinskii, 2006, published in Geokhimiya, 2006, No. 2, pp. 161–166.

Genesis of Ringwoodite during Metamorphism Induced by Impact Waves: Experimental Data

L. V. Sazonova*, V. I. Fel'dman*, E. A. Kozlov, N. A. Dubrovinskaya***, and L. S. Dubrovinskii*****

** Division of Geology, Moscow State University, Vorob'evy gory, Moscow, 119899 Russia*
e-mail: saz@geol.msu.ru, feldman@geol.msu.ru
*** Zababakhin All-Russia Research Institute of Technical Physics, Russian Federal Nuclear Center, Snezhinsk, Russia*
**** Bayerisches Geoinstitut, Bayreuth, Germany*

Received January 10, 2004

Abstract—Ringwoodite, a high-density olivine modification, was first synthesized by loading plagioclase–biotite–quartz schist containing garnet and staurolite by impact waves. Ringwoodite was identified in the impact–thermal aggregates that replaced biotite (together with a mineral corresponding to spinel in chemical composition and with a biotite residue). The physical parameters under which ringwoodite was synthesized in this experiment (P_{imp} ~ 20–30 GPa and T ~ 1060–1500°C) include a pressure approximately 1.5 times higher than that in static analogous experiments. The ringwoodite was formed via the regrouping of and the associated removal and addition of material, as follows from the development of ringwoodite after biotite, a mineral of principally different composition. Component migration was reliably confirmed by the microprobe mapping of the chemistries of the original and newly formed minerals, which makes the origin of the ringwoodite similar to the origin of diamond (togorite) in the Kara astrobleme, where the impact loading was up to ten times higher than the static pressure.

DOI: 10.1134/S0016702906020030

INTRODUCTION

High-density polymorphic modifications of minerals serve as one of the most reliable indications of impact structures (meteorite craters or astroblemes). It was determined in the late 20th century that astroblemes may contain polymorphs of silica (coesite and stishovite), carbon (diamond and lonsdaleite), and orthopyroxene (majorite), but it was not until 2001 that ringwoodite (γ-olivine) was found in pumice from El Gasko in Extremadura, Spain [1]. Simultaneously, ringwoodite was first synthesized by shock-wave loading of plagioclase-biotite-quartz schist with garnet and staurolite [2].

EXPERIMENTAL

The experiment was conducted with plagioclase–biotite–quartz schist containing garnet and staurolite from the target of the Janisjarvi astrobleme [3]. The rock is schistose, porphyroblastic, with a fine-grained lepidogranoblastick groundmass. The major rock-forming minerals are quartz, plagioclase (which account for ~50% of the rock by volume), and biotite (~40%); the minor minerals are garnet and staurolite (no more than 5 vol % each). The two latter minerals occur as porphyroblasts submerged in a fine-grained plagioclase–biotite–quartz matrix. This polymineralic composition of the rock selected for the impact experiment was as close as possible to the composition of natural shock-metamorphosed rocks.

The experiment was conducted at the Zababakhin All-Russia Research Institute of Technical Physics of the Russian Federal Nuclear Center in the town of Snezhinsk. The sample prepared for the experiment was a rock sphere 49 mm in diameter, which was welded into an air-tight stainless-steel (12Kh18N10T) shell and was loaded with spherical converging stress wave. The wave was generated by the explosion of a layer of explosives 10 mm thick (h_{expl} = 10 mm). The sphere was affected by shock pressures ranging from 20 GPa at the surface to 250 GPa within 1 mm from the center over a time span of 1–2 μs. After the experiment, the sphere was quenched at an initial rate of 10^8–10^9°C/s. On the one hand, this ensured the preservation of the newly formed phases and, on the other, precluded the processes of annealing, lower temperature hydrothermal alterations, etc. The temperature and pressure gradients (they increased along the radius with the propagation of the shock wave from the sphere surface toward its center) were calculated following the method elaborated at the Zababakhin All-Russia Research Institute of Technical Physics, Russian Federal Nuclear Center [4], which makes use of the Hugoniot adiabat calculated from the density of the pristine rock and its chemical composition [5]. The VOLNA computer program [6] enables calculating the dependence of the

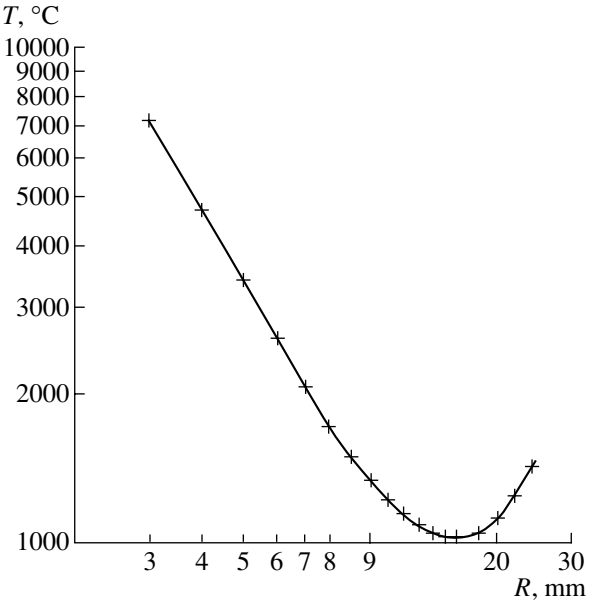

Fig. 1. Dependence of the temperature (*T*, °C) at the shock wave front on the distance (along the radius of the sphere, *R*, mm) of a given point from the center of the sphere [6].

amplitude of the shock stress (*P*, GPa), which has the form $P = 304.7 \times R^{-1.1}$, and the temperature at the shock wave front (*T*, °C) (Fig. 1) as a function of the distance along the radius (*R*, mm) from the sphere center to a specified point.

Upon its shock loading, relaxation, and cooling, the sphere was cut along its meridional plane by a diamond-impregnated circular saw. The polished surface of the cross section was then examined along its radius *R*. The compositions of minerals after their loading by the converging stress wave were analyzed at the Laboratory of High-Resolution Analytical Techniques of the Division of Geology, Moscow State University, on a CamScan-4DV electron microscope equipped with a Link AN-10000 EDS analytical system. The analyses were conducted at an accelerating voltage of 15 kV and a sample current of $(1–3) \times 10^{-9}$ A, accurate to ±2% at elemental concentrations of more than 10 wt %, ±5% at concentrations of 5–10 wt %, and ±10% at concentrations of 1–5 wt %. The excitation area at the sample was equal to approximately 3 μm. The Raman spectra of ringwoodite were obtained on a LabRam spectrometer at the Bayerisches Geoinstitut in Bayreuth, Germany, using a 632-nm laser, 50× lens, and an 1.1-mm confocal slit. The examined region was approximately equal to 7 μm in the focal plane (to a depth of <10 μm into the sample) at a resolution of 2 cm^{-1}.

EXPERIMENTAL RESULTS

The sample affected by shock metamorphism displayed four zones, which could be visually discernible in the polished surface of the sample section. The outermost zone (I) is approximately 12.5 mm thick. The texture of the rock is the same as the texture of the pristine (unmetamorphosed by the shock wave) rock, with sharp boundaries of mineral grains. The pressures in this zone reached 25–20 GPa (increasing toward the sphere center). Chemical alterations of the minerals become discernible only in the part of the zone situated closer to the center of the sphere [7], at different distances from it for each mineral, i.e., at different shock pressures.

The second zone (II) is 5–7 mm thick. The texture of the rock is generally preserved, but the boundaries of mineral grains become diffuse and not as sharp as in the previous zone owing to the diffusion of chemical components during the load impulse. The shock pressures in the inner portion of this zone reached 50 GPa. Zone II is characterized by widespread solid-phase alterations of minerals: amorphization of quartz and plagioclase, the development of shock thermal aggregates (STA) after biotite, garnet, and staurolite. Analogous processes were described in detail for different rocks under similar conditions [7, 8, and others].

The third zone (III) had a width of 2–1.5 mm. The texture of the rock composing this zone was notably modified. The boundaries between mineral grains virtually disappear, giving way to gradual transitions between minerals. This zone corresponded to the onset of selective melting of minerals. The shock pressure in this zone ranged from 50 to 70–80 GPa from the outer to inner boundaries of the zone.

Finally, the fourth zone (IV) at the center of the sphere was characterized by the complete melting of the materials. This zone was 7–9 mm thick and was produced under pressures of >80 GPa. The melt in the zone was not completely homogenized.

It should be mentioned that the boundaries between the zones are drawn fairly arbitrarily because the minerals composing these zones have different chemical compositions, crystal structures, and, as a consequence, analogous shock-induced features (such as amorphization, shock-induced thermal decomposition, and melting) appear in them under different shock pressures. This was described in much detail in [7, 9], with detailed descriptions of the behavior of each mineral.

CHARACTERIZATION OF RINGWOODITE

Ringwoodite was found in the shock thermal aggregates (STA) developing after biotite, mostly in zone II. This mineral appeared already at 20 GPa in the form of rare small (a few micrometers) grains and their aggregates along weakened zones (fracture planes etc., Fig. 2). These aggregates consisted of ringwoodite and spinel of composition close to hercynite, which are submerged in amorphized biotite residue. Ringwoodite

composes small (no more than 20 μm, occasionally as large as 40 μm long and up to 7–8 μm wide) crystals. The crystals are commonly platy, sometimes sheath-shaped (Fig. 3). As the shock pressures increased, the amount of ringwoodite in the shock-metamorphic aggregates after biotite increased, as also increased the elongation L (the length to width ratio) of the ringwoodite crystals. The dependence of the elongation L of ringwoodite crystals on the shock pressure P is expressed as

$$L = -20.5 + 1.1P \text{ at } S = 1.38;\ R = 0.885;\ n = 36,$$

where S is the standard deviation, R is the correlation coefficient, and n is the number of measurements of elongation values at different pressures.

The identification of the mineral with ringwoodite was confirmed by Raman spectroscopy [10, 11] (Fig. 4).

The comparison of the Raman spectra of a ringwoodite standard and the spectra of this mineral from our sample indicates that the latter spectra have a high background, a feature suggesting that the material could include many admixtures. This is corroborated by microprobe analyses of the grains (table). Our ringwoodite pervasively contains some components that are absent from pure olivine (as well as from γ-olivine): Al (up to 9 wt %), Ti, and K (table). These admixtures occur because the ringwoodite was produced via the decomposition of biotite, with some of its components (such as Si, Fe, and Mg) incorporated into ringwoodite, and the rest (Al, K, and Ti) mostly removed outward but partly retained in the newly formed ringwoodite. This is also evident from the comparison of the compositions of the original biotite, ringwoodite, and the residue after biotite decomposition. The compositions of the biotite and biotite residue indicates that the removal of some components from the original mineral was associated with the addition of others: Na and Ca from the plagioclase-bearing matrix of the schists around the biotite grains. The statistical test of the redistribution of components between the ringwoodite and the residue after biotite decomposition reveals that this redistribution is significant only for MgO (which is concentrated in ringwoodite, Fig. 5) and is described by the equation

$$X_{Mg} \text{ in residue} = 26.7 - 0.797X$$

$$\text{at } S = 1.34, \quad R = -0.756, \quad \text{and } n = 9,$$

where S is the standard deviation, R is the correlation coefficient, n is the number of analyses, and X is the MgO concentration (wt %) in ringwoodite.

The redistribution of other components remains fairly random. The removal and addition of components during shock metamorphism are comprehensively described in [7–9].

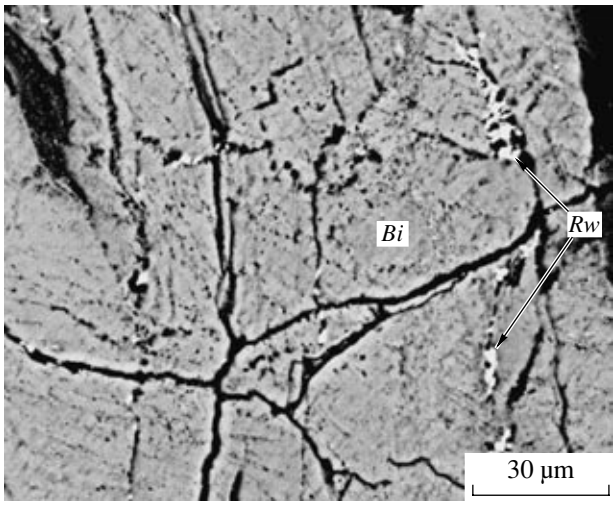

Fig. 2. Biotite (*Bi*) with tiny ringwoodite grains (*Rw*) developing along cracks. P_{shock} = 20 GPa.

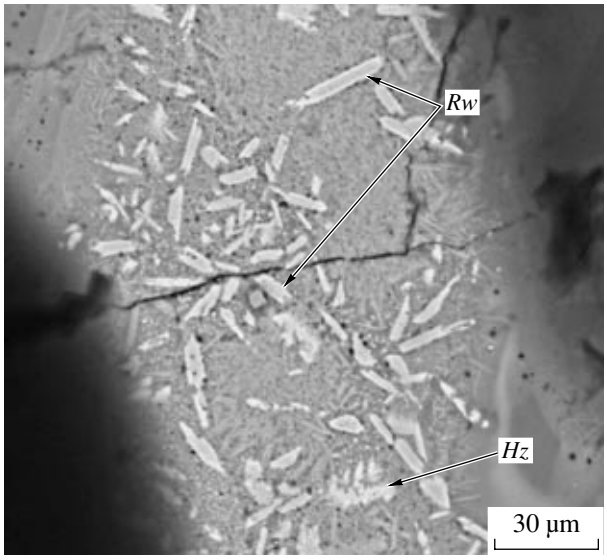

Fig. 3. Shock–thermal aggregate replacing biotite. Aluminous ringwoodite (*Rw*) and hercynite (*Hz*) in the residue after biotite decomposition (gray). P_{shock} = 22 GPa.

CRYSTALLIZATION CONDITIONS OF RINGWOODITE

In spite of the presence of many admixtures, the composition of the mineral is consistent with the formula $Si^{VI}(Fe,Mg)_2O_4$, i.e., spinel of olivine composition whose Si is octahedrally coordinated (in contrast to its tetrahedral coordination in olivine). Al most probably substitutes Si at the octahedrally coordinated site. The high Al_2O_3 concentrations of the mineral (up to

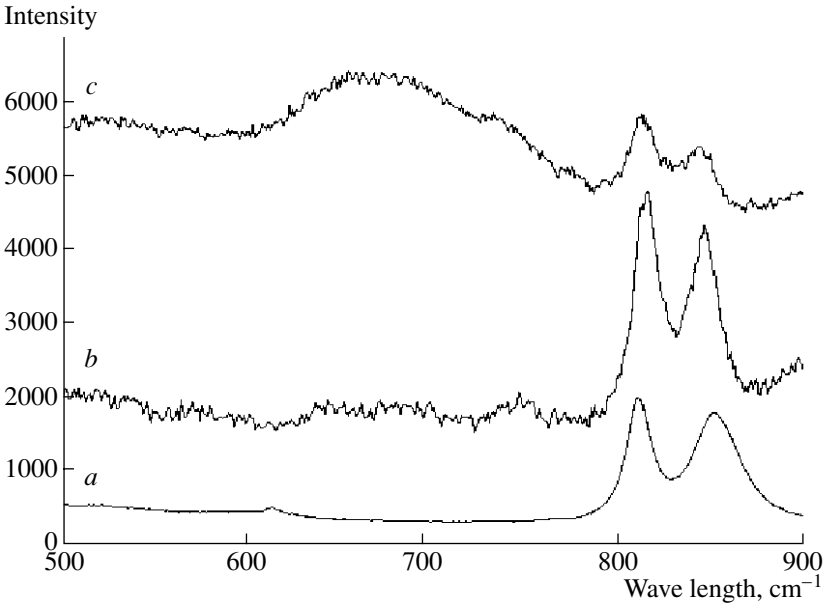

Fig. 4. Raman spectra (500–900 cm^{-1}) of (*a*) ringwoodite synthesized under static conditions, (*b, c*) aluminous ringwoodite synthesized under the effect of a shock wave on plagioclase–biotite–quartz schist (*a*—crystal, point *11*; *b*—crystal, point *17*) [10, 11].

9 wt %) class it with aluminous ringwoodite. Its Fe mole fraction, FeO/(FeO + MgO), ranges within 0.5–0.73. Ringwoodite was produced in this experiment at P_{sh} ~ 20–30 GPa, T ~ 1060–1500°C, which are ~1.5 times higher than the pressure during static loading (no higher than P_{sh} = 21–22 GPa for a comparable composition [12]) (Fig. 6). An analogous tendency of an increase in the parameters of shock metamorphism during stress-wave loading as compared with the static experiment was also documented for the high-density polymorphs of silica [13] and carbon [14–16]. The shock pressure inducing the origin of high-density polymorph modifications also depends on the mechanism of their formation. Now there are three known

Chemical compositions (wt %) of unaltered biotite and phases composing shock-metamorphosed thermal aggregates replacing biotite in zone II

Component	Phase																	
	*Bi**	*Spl***	ringwoodite									residue after biotite decomposition						
	analysis no.																	
	J134	2\47	2\29	11	2\36	2\37	59	72	17	J147	J168	2\31	60	73	J146	J148	J166	J167
SiO_2	36.99	0.41	33.73	32.84	32.41	32.35	33.07	34.00	30.54	33.7	32.5	43.08	43.81	40.69	39.37	41.79	46.45	45.57
TiO_2	2.01	0.48	0.44	0.43	0.91	0.52	0.27	0.20	0.27	0.33	0.39	2.66	2.87	2.71	2.60	1.58	2.38	2.14
Al_2O_3	21.12	60.01	6.00	8.53	0.94	5.14	6.61	3.40	8.92	3.08	7.78	25.96	27.55	23.69	21.83	26.55	25.81	26.64
FeO	22.04	20.82	29.63	28.78	47.54	40.75	29.74	35.12	35.54	37.3	31.2	15.34	12.90	16.27	17.90	15.89	12.36	12.37
MnO	0.00	0.00	0.00	0.00	0.00	0.00	0.00	0.00	0.00	0.00	0.00	0.28	0.00	0.00	0.00	0.00	0.00	0.00
MgO	8.46	14.54	29.68	28.97	17.44	20.75	29.95	27.03	24.29	25.2	27.6	3.74	3.15	7.26	8.46	5.41	2.75	3.06
CaO	0.00	0.00	0.00	0.00	0.14	0.14	0.00	0.00	0.00	0	0.12	1.20	0.59	0.37	0.55	1.21	1.06	1.58
Na_2O	0.00	0.00	0.00	0.00	0.00	0.00	0.00	0.00	0.00	0.00	0.00	1.59	2.58	1.10	1.14	1.86	3.45	3.71
K_2O	9.06	0.00	0.22	0.12	0.11	0.32	0.09	0.00	0.09	0.21	0.12	4.00	5.16	7.56	7.65	5.42	5.17	4.56
*f****	0.72	0.59	0.50	0.50	0.73	0.66	0.50	0.57	0.59	0.59	0.59	0.80	0.80	0.69	0.68	0.75	0.82	0.80

Notes: * *Bi* is the typical composition of unaltered biotite, ** *Spl* is spinel; *** f = FeO/(FeO + MgO) is the Fe mole fraction.

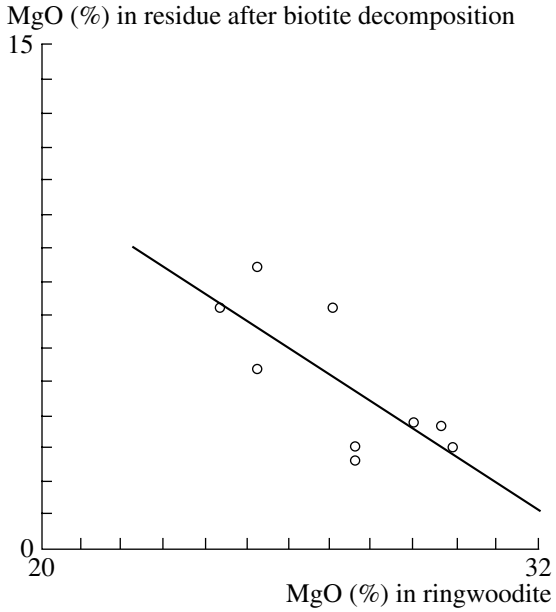

Fig. 5. MgO distribution between aluminous ringwoodite (*Rw*) and the residue after biotite decomposition.

types of these mechanisms: crystallization from a melt, martensite solid-state transition, and the solid-state regrouping of ions coupled with the removal and addition of material [17]. Our experiment evidently reproduced the third mechanism, as follows from the origin of ringwoodite during the decomposition of biotite, a mineral of principally different composition. The migration of components during this process is confirmed by microprobe analyses of the original and newly formed phases (see above), and this makes the origin of the ringwoodite similar to the origin of diamond (togorite) in the Kara astrobleme [18–20], where the dynamic loading exceeded the static pressure by a factor of up to ten.

It is interesting that ringwoodite from Spain [1, 21], which crystallized from an impact melt, differs from this mineral synthesized in our experiment. The crystals of the former ringwoodite are edge forms of skeleton crystals (Fig. 7) and contain fewer admixtures. The melt contains up to 18% Al_2O_3; i.e., the mineral crystallized from a liquid as aluminous as in our experiment (biotite contains 21.12% Al_2O_3). The crystallization conditions of this mineral were 9.5–13.5 GPa and up to 2700°C [21]. Hence, this ringwoodite was produced under the same conditions as other high-density phases. It would be very important to estimate, using olivine, the parameters of the shock-wave load on ringwoodite in order to compare the crystallization conditions under which the former mineral crystallized according to different mechanisms. This is the goal of our further experiments.

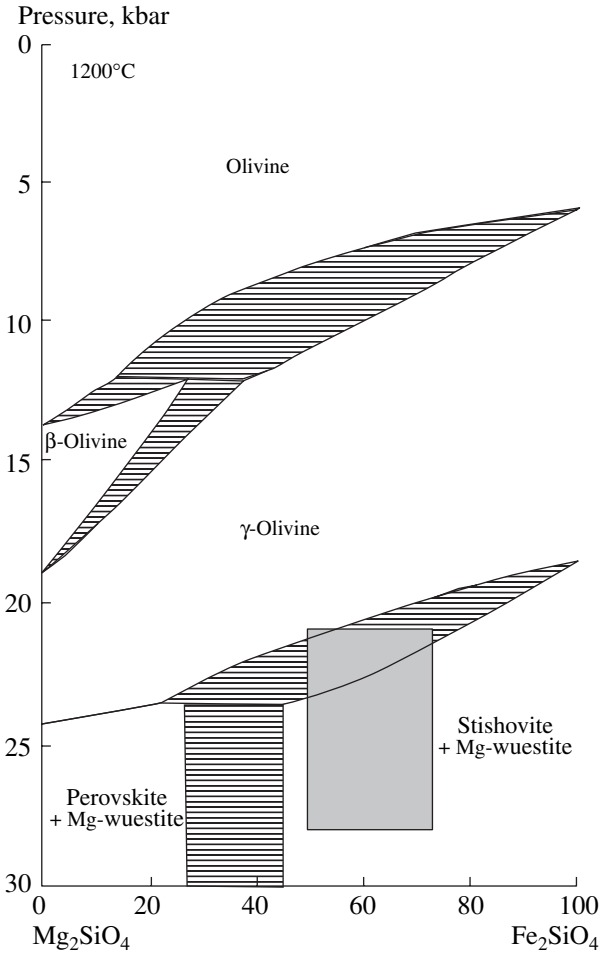

Fig. 6. Stability of olivine polymorphs [12]. The shaded rectangle delineates the stability field of aluminous ringwoodite replacing biotite in our experiment. Fields with horizontal hatching correspond to the coexistence of the phases.

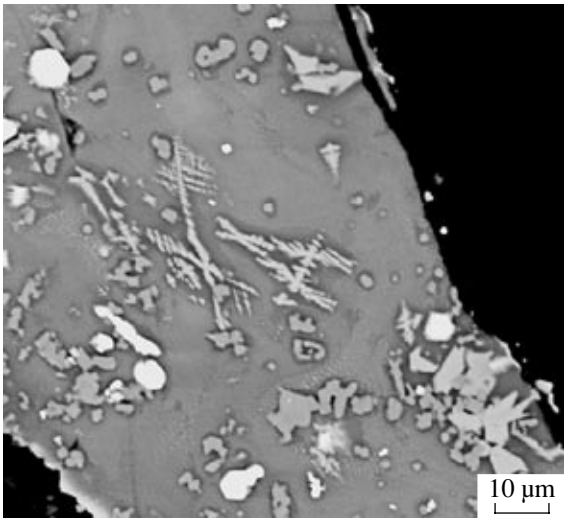

Fig. 7. Edge forms of ringwoodite skeleton crystals (pale gray) in impact pumice from El Gasko, western Spain. White—native iron [21].

CONCLUSIONS

(1) Our experiments were the first to synthesize ringwoodite under the effect of shock wave loading.

(2) This ringwoodite is rich in Al_2O_3 and can be classed with aluminous ringwoodite.

(3) The ringwoodite was formed by the replacement of biotite, a mineral of principally different composition, with the migration of major components but not by means of the martensite transition.

ACKNOWLEDGMENTS

This study was supported by the Russian Foundation for Basic Research, project nos. 03-05-64496, 05-05-64778, and a grant from the President of the Russian Federation for the support of leading research schools (Grant VNSh-1645.2003.5).

REFERENCES

1. E. Diaz-Martinez, E. Sanz-Rubio, C. Fernandez, and J. Martinez-Friaz, "Evidence for a Small Meteorite Impact in Extremadura (W. Spain)," in *Abstracts of 6 ESF-Impact Workshop* (Granada, 2001), pp. 21–22.
2. L. V. Sazonova, V. I. Fel'dman, E. A. Kozlov, and Yu. N. Zhugin, "Impact Metamorphic Migration of Chemical Components of Minerals in the Janisjarvi Astrobleme," in *Abstracts of Papers of the International Conference "The VI Zababakhin Scientific Readings"* (RFYuTs-VNIITF, Snezhinsk, 2001), pp. 171–174 [in Russian].
3. *Impactites*, Ed. by A. A. Marakushev (Mosk. Gos. Univ., Moscow, 1981) [in Russian].
4. E. A. Kozlov, "Studies of Metals, Minerals, and Meteorites in Spherical Impact Isentropic Experiments: A Review of Polymorph and Phase Transformations, Scabbing- and Sliding-Related Destructions, and Physicochemical Transformations," in *Proceedings of the International Conference "The V Zababakhin Scientific Readings"* (RFYuTs-VNIITF, Snezhinsk, 1999), Part 1, pp. 579–590 [in Russian].
5. G. S. Telegin, V. G. Antoshev, V. A. Bugaeva, *et al.*, "Calculation of Impact Adiabats for Rocks and Minerals," Izv. Akad. Nauk SSSR, Ser. Fiz. Zemli, No. 5, 22–31 (1980).
6. V. F. Kuropatenko, G. V. Kovalenko, V. I. Kuznetsova, *et al.*, "The Volna Software Package and the Heterogeneous Difference Method for Calculating Movements of Contractible Medium," Vopr. At. Nauki Tekhn., Ser. Metod. Progr. Chisl. Reshen. Zadach Matem. Fiz., No. 2, 9–25 (1989).
7. L. V. Sazonova, V. I. Fel'dman, E. A. Kozlov, and Yu. N. Zhugin, Preprint No. 198, RFYaTs–VNIITF (Russian Federal Nuclear Center–All-Russia Research Institute of Technical Physics, Snezhinsk, 2002).
8. V. I. Fel'dman, L. V. Sazonova, and E. A. Kozlov, "Mobility of Major Elements during Shock Metamorphism: Experimental Evidence," Dokl. Akad. Nauk **393** (1), 1–3 (2003) [Dokl. Earth Sci. **393A** (9), 1333–1335 (2003)].
9. E. A. Kozlov, Yu. N. Zhugin, B. V. Litvinov, *et al.*, Preprint No. 151. RFYaTs–VNIITF (Russian Federal Nuclear Center, All-Russian Research Institute of Technical Physics, Snezhinsk, 1998).
10. E. Kozlov, L. Sazonova, V. Fel'dman, *et al.*, "Formation of Ringwoodite in High-Explosive Experiments on Muscovite–Biotite–Quartz Slates," in *Annual Report of Bayerisches Forschungsinstitut für Experimentelle Geochemie und Geophysik—Uuniversitat Bayreuth* (Bayerisches Geoinstitut-Uuniversitat Bayreuth, 2002), pp. 100–101.
11. E. A. Kozlov, L. V. Sazonova, V. I. Fel'dman, *et al.*, "Formation of Ringwoodite during the Shock-Wave Loading of Two-Mica Quartz Schist: Experimental Data," Dokl. Akad. Nauk **390** (3), 379–381 (2003) [Dokl. Earth Sci. **390** (4), 571–573 (2003)].
12. *Ultrahigh-Pressure Mineralogy*, Ed. by R. J. Hemley, Rev. Mineral. **37** (1998).
13. B. M. Mitsyuk and L. I. Gorogotskaya, *Physicochemical Transformations of Silica under Metamorphic Conditions* (Naukova Dumka, Kiev, 1980) [in Russian].
14. A. A. Val'ter, G. K. Eremenko, V. N. Kvasnitsa, and Yu. A. Polkanov, *Impact Metamorphic Minerals of Carbon* (Naukova Dumka, Kiev, 1992) [in Russian].
15. S. A. Vishnevskii, V. P. Afanas'ev, K. P. Argunov, and N. A. Pal'chik, *Impact Diamonds: Characteristics, Origin, and Significance* (Ob''ed. Inst. Geol. Geophys. Mineral., Sib. Otd. Ross. Akad. Nauk, Novosibirsk, 1997) [in Russian].
16. V. V. Danilenko, *Explosion-Induced Synthesis and Agglomeration of Diamond* (Energoatomizdat, Moscow, 2002) [in Russian].
17. V. I. Fel'dman, *Petrology of Impactites* (Mosk. Gos. Univ., Moscow, 1990) [in Russian].
18. V. A. Ezerskii, "Shock-Metamorphosed Carbonaceous Matter in Impactites," Meteoritika **41**, 134–140 (1982).
19. V. A. Ezerskii, "Hyperbaric Polymorphs Formed during Shock Metamorphism of Coals," Zap. Vseross. Mineral. O-va, No. 1, 26–33 (1986).
20. V. A. Ezerskii, Extended Abstract of Candidate's Dissertation in Geology and Mineralogy (VSEGEI, Leningrad, 1987).
21. L. I. Glazovskaya, E. Dias-Martines, V. I. Fel'dman, and J. Martines-Frias, "Ringwoodite from Estremadura Pumices, Western Spain: Compositional Features," in *Proceedings of the III International Conference "New Mineralogical Ideas and Concepts"* (Geoprint, Syktyvkar, 2002), pp. 108–110 [in Russian].